

TR7  
W34C  
No. 2-66

WES CONTRACT REPORT 2-66  
RUNOFF FROM IMPERVIOUS  
SURFACES FEB. 1966

AD 730 732

Reproduced by  
**NATIONAL TECHNICAL  
INFORMATION SERVICE**  
Springfield, Va. 22151

RUNOFF FROM IMPERVIOUS SURFACES

by

Y. S. Yu and John S. McNown

Prepared for

WATERWAYS EXPERIMENT STATION

Vicksburg, Mississippi

Under Contract No. DA-22-079-eng-290

Lawrence, Kansas

February 15, 1963

TH7  
W<sup>2</sup>4c  
100, 2-66

## RUNOFF FROM IMPERVIOUS SURFACES<sup>1</sup>

by

Y. S. Yu<sup>2</sup> and John S. McNown<sup>3</sup>

### Resume

Runoff of rain falling on an impervious surface can be predicted by means of numerical computations. For the usually small slopes and depths which occur on highways or airstrips, the non-uniform flow is quasi-steady. Experiments conducted in the Los Angeles District are adequate for the estimation of resistance coefficients for flows which can be laminar or turbulent and rapid or tranquil, with all four conditions occurring simultaneously in some instances. Neither the analysis nor the experiments include cases in which surface disturbances such as roll waves may occur.

The calculation proceeds by steps in the direction of flow, beginning at the upstream end of the reach and with the incidence of rain; repeated computations provide predictions of depths and velocities at subsequent times. Because most of the rain falling is stored on the surface initially, the flow approaches equilibrium quite rapidly. In fact, an acceptable estimate of the time to achieve a flow condition approximating equilibrium is obtained simply by dividing the equilibrium depth by the rate of rainfall. If the rate of rainfall changes, the same set of equations provides information on the transition or recession curve. Other, more complex conditions can be taken into account in a set of computations if the requisite information is available.

---

<sup>1</sup>A study conducted under a contractual agreement with the U. S. Army Waterways Experiment Station, Corps of Engineers, Vicksburg, Mississippi.

<sup>2</sup>Associate Professor, Department of Mechanics and Aerospace Engineering, School of Engineering and Architecture, The University of Kansas, Lawrence, Kansas.

<sup>3</sup>Dean, School of Engineering and Architecture, The University of Kansas, Lawrence, Kansas.

The computations provide results which correspond satisfactorily with hydrographs observed in the Los Angeles field tests for several complete runs, and for parts of other runs. The anomalous increase in discharge which often followed the cessation of rain in these tests is a consequence of turbulent flow becoming laminar when the battering of the rain ceases. The increase does not occur because the flow is no longer retarded by the rain, as originally hypothesized.

More precise determinations of resistance coefficients and fully detailed comparisons of experimental and theoretical results are not possible because the accuracy of the requisite measurements is well beyond ordinary methods, however carefully performed. The lack of precision is not important in practice because the occurrence of rain in nature is so variable. Acceptable predictions can be made from the data provided by the Los Angeles tests and with the method of computation proposed. The refinement obtained in these tests is also sufficient for the explanation of the primary characteristics of the flows.

#### Experimental Program of the Los Angeles District

During the period from 1948 to 1954, the Los Angeles District of the Corps of Engineers conducted an extensive experimental study of air field drainage at Santa Monica, California. The purpose of the investigation was to determine by means of controlled experiments certain aspects of the relationship between rainfall and runoff from both paved surfaces and from surfaces which simulate turf. Simulated rainfall caused runoff from any of three separate concrete channels, each 500 ft long and 3 ft wide, and with slopes of 0.5%, 1.0%, and 2%, respectively. Various combinations of rainfall intensity, slope, length of channel, and surface roughness led to a variety of flow patterns. Steady, uniform flows without rainfall provided information as to the resistance characteristics of various types of surface roughness such as concrete pavement, natural grass, and simulated turf. The rainfall intensity ranged from 1/4 to 10 in. per hr. The experimental data include 601 runoff hydrographs and 153 depth hydrographs<sup>4</sup> which

---

<sup>4</sup>"Data Report, Airfield Drainage Investigation", prepared by the Los Angeles District, Corps of Engineers, U. S. Army, October 1955.

a firm of consulting engineers reviewed in 1955.<sup>5</sup> The review was not conclusive, and contained a recommendation for further analysis. Keulegan<sup>6</sup> discussed the equations governing spatially variable flow, and Izzard<sup>7</sup> applied these equations to the computation of the surface profiles at equilibrium state and compared them with measurements. Woo and Brater<sup>8</sup> studied various aspects of the equilibrium state.

Numerous investigators have studied the laws of resistance to flow in small open channels. Among the more recent are Owens<sup>9</sup>, Iwagaki<sup>10</sup>, Woo and Brater<sup>11</sup>, and Straub et al<sup>12</sup>. Experimental evidence indicates that, even in laminar flow, the resistance depends on the surface roughness, as well as on the channel slope, the channel cross section, and the rainfall intensity. Woo and Brater found that for a masonite surface with the rough side up the resistance coefficient is given by  $f = 30.8/R$ , an equation which yields larger values than does the generally accepted equation for smooth surfaces. For a sand-coated surface, they found the constant  $C$  to vary significantly with the slope. They also observed some effect of rainfall on resistance

---

<sup>5</sup>"Review of data report on airfield drainage investigation", by Dodson, Kirney and Lindblom, Consulting Engineers, October 1955.

<sup>6</sup>Keulegan, G. K., "Spatially variable discharge over a sloping plane", Trans. AGU, Vol. 25, pp. 956-959, 1944.

<sup>7</sup>Izzard, C. F., "The surface profile of overland flow", Trans. AGU, Vol. 25, pp. 959-968, 1944.

<sup>8</sup>Woo, D.C., and Brater, E.F., "Spatially varied flow from controlled rainfall", Proc. ASCE Vol. 88, No. H.Y. 6, Part 1, pp. 31-56, Nov. 1962.

<sup>9</sup>Owen, W.M., "Laminar to turbulent flow in a wide open channel", Trans. ASCE Vol. 119, pp. 1157-1175, 1954.

<sup>10</sup>Iwagaki, Y., "On the laws of resistance to turbulent flow in open channels", Proc. 4th Japan Nat. Cong. Appl. Mech., pp. 229-233, 1954.

<sup>11</sup>Woo, D.C. and Brater, E.F., "Laminar flow in rough rectangular channels", Jr. Geophys Res., Vol. 66, No. 12, pp. 4207-4217, Dec. 1961.

<sup>12</sup>Straub, L.G., Silberman, E., and Nelson, H.C., "Open channel flow at small Reynolds numbers", Trans. ASCE Vol. 123, pp. 685-714, 1958.

for three rainfall intensities and over a limited range of Reynolds number. The variation of  $C$  with roughness is inconsistent with the generally accepted premise that the laws of laminar flow apply equally to rough and smooth surfaces. However, the relative roughness of flow in thin sheets over a rough surface can be so high as to result in inconsistencies if usual definitions of these quantities are used. In the work cited,<sup>11</sup> the roughness was a significant fraction of the depth in some cases; the velocity distribution must surely have been affected.

In the Los Angeles experiments, sprinklers supplied an artificial and uniform rainfall over an entire channel, and an ogee-shaped weir in a weir box, which was placed five feet downstream from the end of the channel, made possible the measurement of the runoff. A float in the stilling well of the weir box, connected to an electric recorder, registered the variation of the head on the weir. A volumetric tank served for the calibration of the weir. The effect of storage in the weir box is negligible as shown in the Los Angeles District report<sup>4</sup>. The report also contains details of the instruments and the procedures followed in measuring the depth both in gage wells and directly over the channel to an accuracy of a few ten-thousandths of a foot.

Depth and discharge measurements for steady, uniform flow without rainfall supplied data for the determination of values of the resistance coefficient  $f$ , which is equal to  $8gSh/u^2$  \*. Figure 1 contains the resulting resistance coefficients for the concrete surface plotted against the Reynolds number ( $R = uh/\nu$ ). The experimental points, which include only a limited range of Reynolds number, indicate much higher resistance coefficients than those for a smooth flat plate. Due to lack of experimental data in the transition region, the curve which connects the mean curve for turbulent flow and the laminar resistance curve ( $f = 24/R$ ) was drawn somewhat arbitrarily. A similar curve in Fig. 2 presents data obtained in the steady-state runs with rainfall. Although the data are rather scattered, the corresponding resistance coefficients in the transition region are clearly higher with rain than those for flow without rain. The few exceptionally low points in Fig. 2 were ignored because most of them occurred for one piezometer (that at  $x = 333$  feet in

---

\* Symbols are defined in Appendix 1

the No. 1 channel with a slope of 0.5%). The curves drawn in Figs. 1 and 2 constitute the resistance relationships used in computing runoff hydrographs. Because of the foregoing somewhat arbitrary decision, the two curves differ only in the transition region,  $200 < R < 1000$ .

Data for flow over simulated turf surfaces with three different slopes are plotted in Fig. 3 for flow both with and without rainfall. The scatter of points is great but the effect of slope on the resistance coefficient is unobscured. The points for  $S = 0.010$  and  $0.020$  are close but the points for  $S = 0.005$  fall significantly below those for  $S = 0.020$ . Therefore two straight lines are drawn in the figure, one for  $S = 0.005$  with  $C = 56.6$  and  $n = 0.687$  in  $f = C/R^n$ , and the other line for both  $S = 0.010$  and  $0.020$ , with  $C = 117$  and  $n = 0.681$ . These values are again somewhat arbitrary.

### Analysis

The one-dimensional equation of motion for the runoff of rain which falls on an impervious surface (with reference to Fig. 4) is as follows:

$$\frac{\partial u}{\partial t} + u \frac{\partial u}{\partial x} = g(S - \frac{\partial h}{\partial x}) - \frac{\tau}{\rho h} - \frac{u \sigma}{h}. \quad (1)$$

in which  $\tau$  is the shearing stress at the boundary,  $\sigma$  is the rainfall intensity;  $\rho$  is the mass density of water,  $h$  is the depth of water and  $u$  is the average velocity at a section. The two terms on the left side of Eq. (1) are the local and the convective accelerations. The forces acting on a unit mass, on the right side, are those due to gravity, boundary shear, and the retarding effect of the rainfall. The slope of the boundary is usually small enough in any practical application to justify the usual approximations for small angles.

The equation of continuity,

$$\frac{\partial(uh)}{\partial x} = \sigma - \frac{\partial h}{\partial t}, \quad (2)$$

relates the rate of change of discharge along the channel to the difference between the rate of rainfall and the rate of storage. In general,  $u$ ,  $h$ ,  $\tau$  and  $\sigma$  in Eqs. (1) and (2) depend on both time and distance. For a known rate of rainfall, three unknown quantities remain in the two equations. The additional information needed to complete the analysis is an empirical relationship between  $f$  and  $R$  such as Fig. 1, 2, or 3.

The initial condition for the tests, a dry channel and no rainfall, described mathematically, are  $u = 0$ ,  $h = 0$  at  $t < 0$  for  $0 \leq x \leq L$ . The boundary conditions at the upstream end is  $u = 0$  for  $t \geq 0$ , but the depth  $h$  at this point can change with time. For simplicity in the computation, the value of  $h$  at  $x = 0$  is taken to be the same as that at  $x = \Delta x$ . Since both the upstream depth and the channel slope are small, the effects of the error implicit in this assumption and of ignoring the small pool of water which forms upstream from  $x = 0$  are negligible.

If the rain is uniformly distributed and falls at a constant rate, the motion soon becomes steady. The term  $\partial u / \partial t$  is then zero in Eq. (1), and  $\partial h / \partial t$  is zero in Eq. (2). If the rain stops,  $\sigma$  becomes zero in both equations.

For the useful range, represented by the range of the tests conducted by the Los Angeles District, the orders of magnitude of the terms in Eqs. (1) and (2) differ greatly. One finds that four terms - the two accelerated terms, the term describing changes in depth  $g(\partial h / \partial x)$  and the term accounting for the deficiency in momentum of the falling rain - are each less than 1/100 of the other gravitational term and the term for resistance. If these terms are omitted and if  $fu^2/8$  is substituted for  $\tau/\rho$ , Eq. (1) reduces to

$$h = \frac{\tau}{\rho g S} = \frac{fu^2}{8gS}, \quad (3)$$

simply the resistance equation for steady, uniform flow. The flow is therefore quasi-steady and locally uniform. The orders of magnitude of

all three terms in Eq. (2) can be the same, so all enter into the computation. From this examination, one concludes that Eqs. (2) and (3), together with the resistance curves and the initial and boundary conditions, constitute an adequate basis for numerical determinations of the depth and the velocity (or the discharge) as functions of time and distance.

The first step in the computation is the determination of  $h$  and  $u$  for equilibrium conditions from Eqs. (2) and (3). Since  $\sigma$  is known, the discharge per foot of width,  $uh$ , at any section comes from Eq. (2). The Reynolds number at the section is then known for an appropriate value of the kinematic viscosity  $\nu$ , and the resistance coefficient  $f$  is available from Fig. 2. The simultaneous solution of Eqs. (2) and (3) then supplies a pair of values for the depth and the velocity at the section. These values are the limits for the initial transient stage, and occur if the rain persists long enough for steady flow to occur.

The results for the transient flows are calculated by means of a step method based on a finite difference form of Eq. (2).

$$uh = \left( \sigma - \frac{\Delta h}{\Delta t} \right) \Delta x + u_0 h_0, \quad (4)$$

in which  $\sigma$  is a constant, and  $\Delta x$  and  $\Delta t$  are arbitrarily selected intervals of distance and of time. The computation in the  $x-t$  plane begins at the origin,  $x = 0$ ,  $t = 0$ , and proceeds first in the  $x$ -direction. For a given  $\Delta t$ , a trial-and-error procedure is necessary only for the first pair of values of  $u$  and  $h$  which satisfy Eqs. (3) and (4) and the graphical relationship between  $f$  and  $R$ . For the first  $x$ -step from  $x = 0$  to  $x = \Delta x$ , the flow entering the section is zero. One assumes a value of  $\Delta h$ ; computes trial values of  $q$ ,  $u$  and the Reynolds number; sets  $h = \Delta h$  in the first time interval, obtains the resistance coefficient from Fig. 2 for the trial value of the Reynolds number; and computes another value of  $u$  from Eq. (3). If these two values of  $u$  are not acceptably close, he assumes a better value for  $\Delta h$  and repeats the process until sufficiently accurate results are obtained for the initial step.

The value of  $\Delta h$  determined for the first  $x$ -step is an acceptable approximation to the value of  $\Delta h$  to be used for the next  $x$ -step without subsequent trials. Because  $u_0 h_0$ , the flow entering the section from upstream, is also known from the previous  $x$ -step, the computation of  $u$  and  $h$  is also direct. The process is then repeated for subsequent  $x$ -steps until either (a) the value of  $\Delta h/\Delta t$  is equal to  $\sigma$ , or (b)  $x = L$ . The rate of rainfall,  $\sigma$  is a proper upper limit for the value of  $\Delta h/\Delta t$  even though small inaccuracies in the computational procedure can cause the rate of rise to exceed the rate of rainfall. The same step computation along  $x$  provides results for subsequent time steps, and is continued until the flow rate at  $x = L$  is essentially equal to the steady-state discharge (98% of  $\sigma L$  in these computations).\* The resulting grid of values for  $u$  and  $h$  as functions of  $x$  and  $t$  is a complete account of the rising branch of the depth and the runoff hydrographs. Also, at a given time the surface detention can be readily computed from the known depth profile.

Steady, non-uniform flow will persist until a change in the rate of rainfall brings about another transient stage. The step method explained in the preceding section is again applicable. If the rain stops, the recession branch of a hydrograph is just another case with  $\sigma = 0$ , but the values of  $f$  are obtained from Fig. 1, instead of from Fig. 2.

#### Comparisons of Analysis and Experiment

Computations of the depth and the runoff hydrographs for four cases with different combinations of slope, roughness and rainfall form the basis for a comparison between theoretical and experimental results. The following four cases represent quite diverse conditions of flow.

Case 1 - concrete surface, rainfall intensity = 7.44 in/hr,  
 slope = 0.02  
 L = 500 ft.

---

\* Computation was done on the IBM 1620 of the U. S. Army Engineer District, Kansas City, Missouri.

Case II - concrete surface, rainfall intensity = 1.98 in/hr,  
 slope = 0.005,  
 L = 500 ft.

Case III - simulated turf surface, rainfall intensity = 2.00 in/hr,  
 slope = 0.005,  
 L = 500 ft.

Case IV - concrete surface, initial rainfall intensity =  
 1.7 in/hr increases to 3.77 in/hr at  $t = 6$  min, de-  
 creases to 1.75 in/hr at  $t = 18$  min, and ceases at  
 $t = 32$  min.  
 slope = 0.005,  
 L = 252 ft.

Figures 5 and 6 contain the computed and the measured hydrographs for Case I, Figs. 7 and 8 for Case II, Figs. 9 and 10 for Case III, and Fig. 11 for Case IV. The runoff hydrographs were measured at the end of the channel only, and the depth hydrographs were obtained at the various stations indicated in the figures.

These sets of curves follow a consistent pattern. Both depth and runoff increase monotonically with time after the rainfall starts, and closely approximate steady flow after a period of time. The computed curves reach steady state quite rapidly even though their approach is asymptotic; the method used for the step computation exaggerates somewhat the rapidity of this approach toward the limiting condition. After the rain stops, both the depth and the runoff decrease monotonically in Case I, as one would expect. However, in Cases II and IV and in many other cases the measured runoff (Figs. 7 and 11) rises rather quickly to a peak rate appreciably greater than the equilibrium rate before beginning the regular decrease. The pip is seen in Fig. 11, but is not seen in the computed curve shown in Fig. 7. In the latter case the time step ( $\Delta t = 60$  sec.) taken in the computation of the recession branch in the former was too large to reveal this detail. The computation of this kind of peak, for another, more striking case is presented in the following section, and shows clearly the cause and predictability of this anomaly. The pips shown in the measured depth hydrographs at  $x = 467$  ft and 167 ft in Fig. 8 are inconsistent with the flow condition and cannot be explained except possibly on the basis of experimental error.

The computed curves shown in Figs. 9 and 10 for the simulated turf surface correspond well with the measured runoff and depth hydrographs. The results of the Los Angeles experiments for a two-step function for the rainfall intensity yield the type of superpositions of runoff shown in Fig. 11 which one would expect. Again the overall correspondence is good. The discrepancy in the first few minutes of the rising branch is probably due to inaccuracies of discharge measurements in this interval.

The time to wet a dry surface and the time for the water front to travel the five feet through the collecting channel and then through the weir tank undoubtedly caused a delay of some seconds between the commencement of rain and the first recorded runoff, as shown in Figs. 5 and 7. As a consequence, the rising branch of the measured hydrographs lags behind the corresponding computed curves. A similar but probably smaller lag also exists in the runoff hydrograph after the rain stops. During steady flow, the discharge at any section  $x$  is simply  $\sigma x$ . Therefore, the measured and the computed runoff should be the same. They are almost equal but not quite. In Fig. 5, the measured steady runoff is about 0.5% less than the computed value, and in Fig. 7, the measured steady runoff is about 2% higher than the computed value. These discrepancies in steady state discharge occur between the specified rainfall and the observed steady runoff, rather than between prediction and observation.

In the early stages of the establishment of flow, most of the rain goes into storage on the surface so that the initial rate of increase of depth is approximately equal to the rate of rainfall  $\sigma$ . The rate of change of depth subsequently decreases, of course, as runoff begins, and becomes zero when steady flow is established. The slope  $\Delta h/\Delta t$  of the rising branch of the depth hydrograph should never exceed the rate of rainfall, and initially the slopes of the depth hydrographs taken at different stations along the channel should be nearly the same as in the computed curves in Fig. 8. In fact,  $\Delta h/\Delta t$  does exceed  $\sigma$  significantly in some intervals, a condition which is inconsistent with the conditions of flow as already stated. Also, in Fig. 8, the measured steady-state depth at  $x = 333$  ft is considerably below the computed value, whereas those at the other two stations correspond rather well with the computed values. Readings of the depth obtained from this piezometer in

the No. 1 channel (0.5% slope) were consistently low, as stated in a preceding section.

In spite of evidence of imperfections in the experiments, the computed runoff hydrographs based on the simplified analysis correspond surprisingly well with the measured curves. The computed depth hydrographs correspond somewhat less well. For Case 1, the recession branch of the computed depth hydrograph is higher than the measured curve, and the discrepancy increases with time, an inconsistency for which the cause is not known.

A point of qualitative correspondence in the recession branches of the computed and measured hydrographs in Figs. 5 and 7 is the point of inflection and bump which occur sometime after cessation of rain. The corresponding Reynolds numbers indicate that the change is related to the transition from turbulent to laminar flow.

#### The Anomalous Pip on the Runoff Hydrograph

On many of the runoff hydrographs, as mentioned in the preceding section, the discharge increases immediately after the rain stops in a manner shown in Fig. 12. The disturbance caused by the raindrops, not the momentum effect described by Eq. (1), is the reason for this intriguing effect. Although the rain does enter the stream with no net momentum in the direction of flow, and thus retard the flow, the magnitude of the retardation is so small that its cessation could not cause this rather dramatic occurrence. The pips occur primarily for flows in which the Reynolds number can be either laminar or turbulent. Evidently, the falling rain causes flows which would otherwise be laminar to become turbulent. The good correspondence of observation and prediction in Fig. 12 supports this hypothesis.

The heights of those pips which occurred among the 150 runoff hydrographs, obtained in the concrete channels with uniform rainfall, is rather loosely dependent upon the Reynolds number at the end of the channel ( $\sigma L/\nu$ ) as shown in Fig. 13. The Reynolds number in the plot varies from about 100 to 7600, and the maximum relative height of the pip observed is over 20% of the equilibrium discharge, a surprisingly large change. No pips occurred for Reynolds numbers larger than 2200 nor

less than 150. In contrast, pips always occurred for Reynolds numbers between 350 and 1150. Clearly, the pip is related to a transition from turbulent to laminar flow near the downstream end of the channel. No simple relationship exists because the Reynolds number varies along the channel and the degree of disturbance depends also on the rate of rainfall and the depth.

The data in Figs. 1 and 2 indicate a significant effect of rain on the resistance coefficient in the transition region despite their considerable scatter. Thus when the rain ceases and the turbulent flow becomes laminar, the corresponding resistance reduces considerably. The rate of flow is higher than the equilibrium rate for a brief period because the velocity increases more than the depth decreases; the extra flow must come, of course, from storage. If a zone of turbulent flow close to the discharge measuring station becomes laminar, a pip shows on the discharge hydrograph. If the transition is farther upstream, the normal draw-down effect will cause a decrease in discharge which the local increase can not offset. The pip may occur at some point upstream without affecting materially the flow at the downstream end of the channel. The resistance in the fully turbulent region is essentially the same with and without rain; consequently, no pip occurs for these large Reynolds numbers.

Because of the scatter in Figs. 1, 2, and 13, the foregoing explanation is plausible rather than conclusive. The experimental data follow rather consistent trends for a given set of experimental conditions. For example, the black points on Fig. 13 represent two similar runs with almost equal rainfall intensities (1.85 in/hr and 1.87 in/hr for  $L = 168$  ft and  $S = 0.5\%$ ). The relative heights of the two pips are 21% and 15%. These computed values depend on the difference between the peak discharge and equilibrium discharge which is only a few ten thousandths of a cubic foot per second per foot of width compared to an accuracy of measurement of only 0.0001 cfs/ft; better correspondence should not be expected. Thus, even though individual items are insufficiently precise to be convincing, a variety of experimental evidence supports the foregoing explanation of the occurrence of the pips.

### Discussion of Procedure and Results

The foregoing detailed analysis and the comparisons with experiment reveal both the utility of the computational methods employed and limitations on their applicability. The technique developed makes possible the prediction of runoff for a variety of circumstances. Also, the computations can include effects due to variations of rainfall, slope and roughness, or to additional factors such as wind and infiltration. The justification for further complication of the computational process depends upon both the utility of the additional information and the reliability of the supporting information.

Certain quite elementary simplifications are usually justifiable. One of these is the reduction of the problem to one of quasi-steady, locally-uniform flow for the establishing of a relationship between the resistance coefficient and the Reynolds number. The depths are usually small and approach the values for steady flows quite rapidly. In fact, the equilibrium depth divided by the rate of rainfall yields a time at which the depth is probably between 80 and 95% of the equilibrium depth - often an acceptably close approximation to the time to reach equilibrium.

An estimate of the time required to reach equilibrium also serves the function of providing a time scale. The selection of a value for  $\Delta t$  depends on the accuracy which can be justified and on the length of the period being studied. A value as great as one fifth of the equilibrium time is so long as to distort the calculations; a value smaller than one twenty-fifth would probably increase the total amount of work unjustifiably. Also, if the detailed variation of a part of a hydrograph is to be determined, then  $\Delta t$  must be small enough to meet the special requirement. For example, in the computation of the pip,  $\Delta t$  was 15 sec. in comparison to a time of concentration of 16 min. The appropriate value for  $\Delta x$  appears to bear about the same relationship to  $L$  as  $\Delta t$  does to the equilibrium time. The values of  $\Delta x$  used (17, 25, and 33 feet, or about  $L/20$ ), proved to be satisfactory in the computations presented herein.

In some instances, the values of  $\Delta x$  affects indirectly the value of the resistance coefficient used in the step computation. If for  $\sigma = 0$

the Reynolds number of the step is in the transition region, Fig. 1, a large value of  $\Delta x$  could cause a significant change in  $R$ ,  $f$  and consequently in  $h$ . This abrupt change of  $h$  would then propagate along both  $x$  and  $t$ .

Analysis of the results of the experiments with sheet flow conducted by the Los Angeles District indicates that refinement to the degree of relative accuracy usually attainable in controlled tests would require a precision of construction which is impracticably difficult to attain. For depths which are less than a few hundredths of a foot, carefully prepared concrete surfaces are probably less like a smooth slab than they are like a series of depressions and rapids characteristic of a river. The experimenters pointed out the difficulties they encountered, writing for example of "bird baths" which remained after the slabs were drained. Since one infers therefore that regions existed in which the slope was zero or negative, local values for the slope must have varied by as much as  $\pm 100\%$ . From another point of view, the precision of local elevations required to maintain an accuracy of only 10% of the depth for a  $\Delta x$  of one foot (a reach which is many times the depth) is 0.0005 ft for the flattest slope used (0.5%). Achievement of such a precision in a concrete slab over a distance of 500 feet would be exceedingly difficult. The desired accuracy of measurement of the depth was also difficult to achieve. The data for individual piezometers are inconsistent, not on an absolute scale, because the errors are remarkably small, but on a scale relative to the depths and slopes which must be computed or predicted.

The plots of the uniform flow used for determinations of the resistance coefficients are additional evidence of the difficulties encountered in experiments of this kind; and the simulated rainfall made the results even more erratic. Undoubtedly, both the depth and the slope varied considerably from place to place. Fortunately, the averaging of these effects in both time and distance provides results which are acceptably consistent. In spite of the extreme difficulties encountered in the experiments and the evident inconsistencies in some details, the overall results are significant. None of the inevitable flaws prevents the primary and essential results from showing up clearly

and consistently. For example, the refinements achieved by the experimenters to show both the existence of pips at the cessation of rainfall and their cause in the transition from laminar to turbulent are remarkable. Furthermore these results were obtained for flows which could also be in transition between sub- and super-critical velocities. If further refinements are required, they should probably be sought through the conduct of controlled laboratory tests on comparatively short sections of precisely plane surfaces. The techniques of construction and measurement would have to be more precise than the usual ones by factors of perhaps ten. The results would undoubtedly provide additional insights into details of such flows, but would probably not increase one's ability to predict runoff from surfaces constructed in the field.

### Conclusions

Numerical procedures form a basis for predicting the runoff from impervious surfaces which accords satisfactorily with the results of extensive field studies undertaken by the Corps of Engineers around 1950. The equations of continuity and of steady, uniform flow are sufficient if information is also available as to the surface resistance. The proposed equations are simpler than originally expected because a number of otherwise complicating terms are negligible for flow in thin sheets. A program is available in order to make computations on an IBM 1620 computer.

Because the depths are small for the cases studied, otherwise unimportant irregularities affect significantly the accuracy of the experimental results. The available data on resistance scatter considerably even though they do define a useful mean value. The predicted and observed trends for the variations of depth and discharge nevertheless correspond remarkably well. Even the pip, an increase in flow immediately following the cessation of rainfall, is predictable. It results from the change to the laminar state of a flow which had formerly been made turbulent by the battering of rain drops. The technique of computation proposed is surely adequate for the design of airfields and highways provided that slopes are not so great as to cause roll waves. Further refinements either of the theory or of the experiments are probably not justifiable on pragmatic grounds. The vagaries of the design storm and of the structure make a more rigorous design impractical.

## APPENDIX I

## LIST OF SYMBOLS

- C - Constant coefficient.  
 f - Resistance coefficient.  
 g - Gravitational acceleration,  $\text{ft}/\text{sec}^2$ .  
 h - Local water depth, ft.  
 L - Total length of surface subjected to rainfall, ft.  
 n - Exponent  
 q - Local discharge per foot of width,  $\text{cfs}/\text{ft}$ .  
 $q_e$  - Equilibrium discharge  
 $\Delta q$  - Maximum increase in discharge after cessation of rainfall.  
 S - Slope of surface  
 t - Time, sec.  
 u - Velocity in x-direction, average over section,  $\text{ft}/\text{sec}$ .  
 x - Distance measured in direction of flow, ft.  
 R - Local Reynolds number defined as  $uh/\nu$ .  
 $\nu$  - Kinematic viscosity of water,  $\text{ft}^2/\text{sec}$ .  
 $\rho$  - Mass density of water,  $\text{slug}/\text{ft}^3$ .  
 $\sigma$  - Rainfall intensity,  $\text{ft}/\text{sec}$  or  $\text{in}/\text{hr}$ .  
 $\tau$  - Boundary shear stress,  $\text{lb}/\text{ft}^2$ .

## APPENDIX II

## LIST OF FIGURES

- Fig. 1 Resistance to Sheet Flow on a Concrete Surface Without Rainfall.
- Fig. 2 Resistance to Sheet Flow on a Concrete Surface With Rainfall.
- Fig. 3 Resistance to Sheet Flow on a Simulated Turf Surface.
- Fig. 4 Definition Sketch.
- Fig. 5 Runoff Hydrographs, Case I,  $S = 2\%$ ,  $\sigma = 7.44$  in/hr.
- Fig. 6 Depth Hydrographs, Case I,  $S = 2\%$ ,  $\sigma = 7.44$  in/hr,  $x = 467$  ft.
- Fig. 7 Runoff Hydrographs, Case II,  $S = 0.5\%$ ,  $\sigma = 1.98$  in/hr.
- Fig. 8 Depth Hydrographs, Case II,  $S = 0.5\%$ ,  $\sigma = 1.98$  in/hr.
- Fig. 9 Runoff Hydrographs, Case III,  $S = 0.5\%$ ,  $\sigma = 2.00$  in/hr, Simulated Turf Surface.
- Fig. 10 Depth Hydrographs, Case III,  $S = 0.5\%$ ,  $\sigma = 2.00$  in/hr,  $x = 467$  ft, Simulated Turf Surface.
- Fig. 11 Runoff Hydrographs, Case IV,  $S = 0.005$ ,  $x = 252$  ft.
- Fig. 12 An Example of a Pip on Runoff Hydrograph,  $S = 0.5\%$ ,  $\sigma = 0.851$  in/hr.
- Fig. 13 Relative Height of Pip as a Function of Reynolds Number.

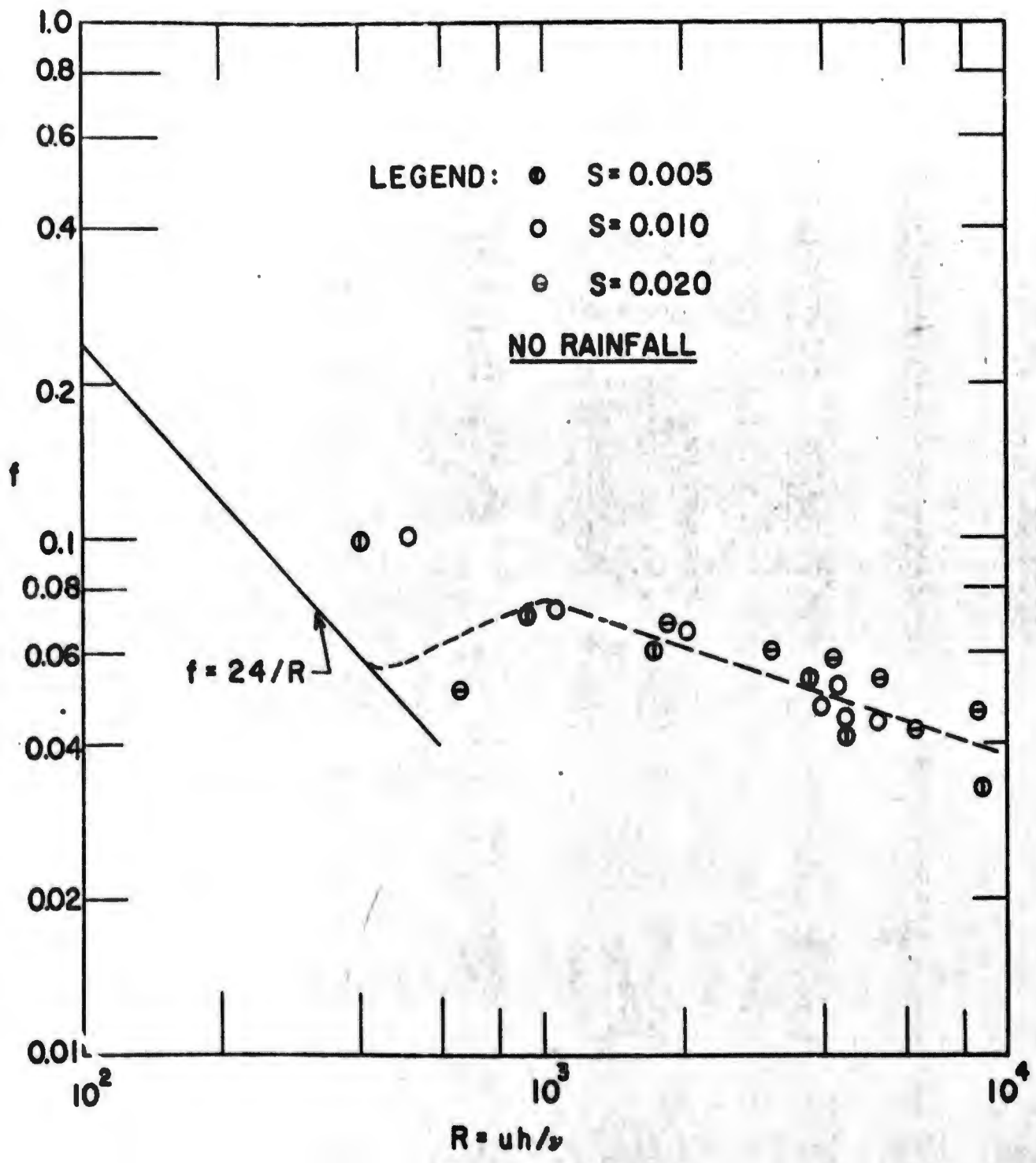


FIG. 1 RESISTANCE TO SHEET FLOW ON A CONCRETE SURFACE WITHOUT RAINFALL

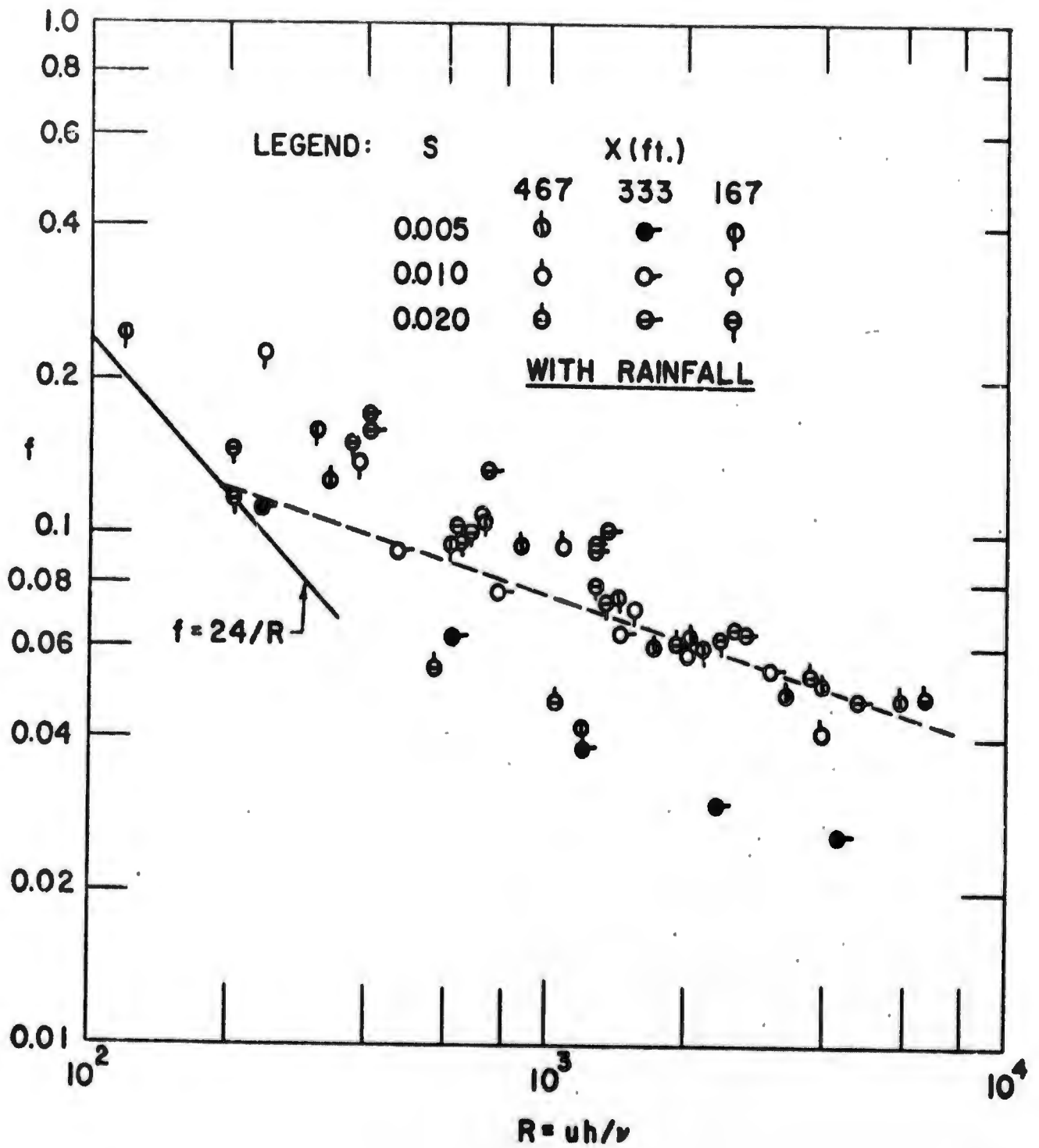


FIG. 2 RESISTANCE TO SHEET FLOW ON A CONCRETE SURFACE WITH RAINFALL

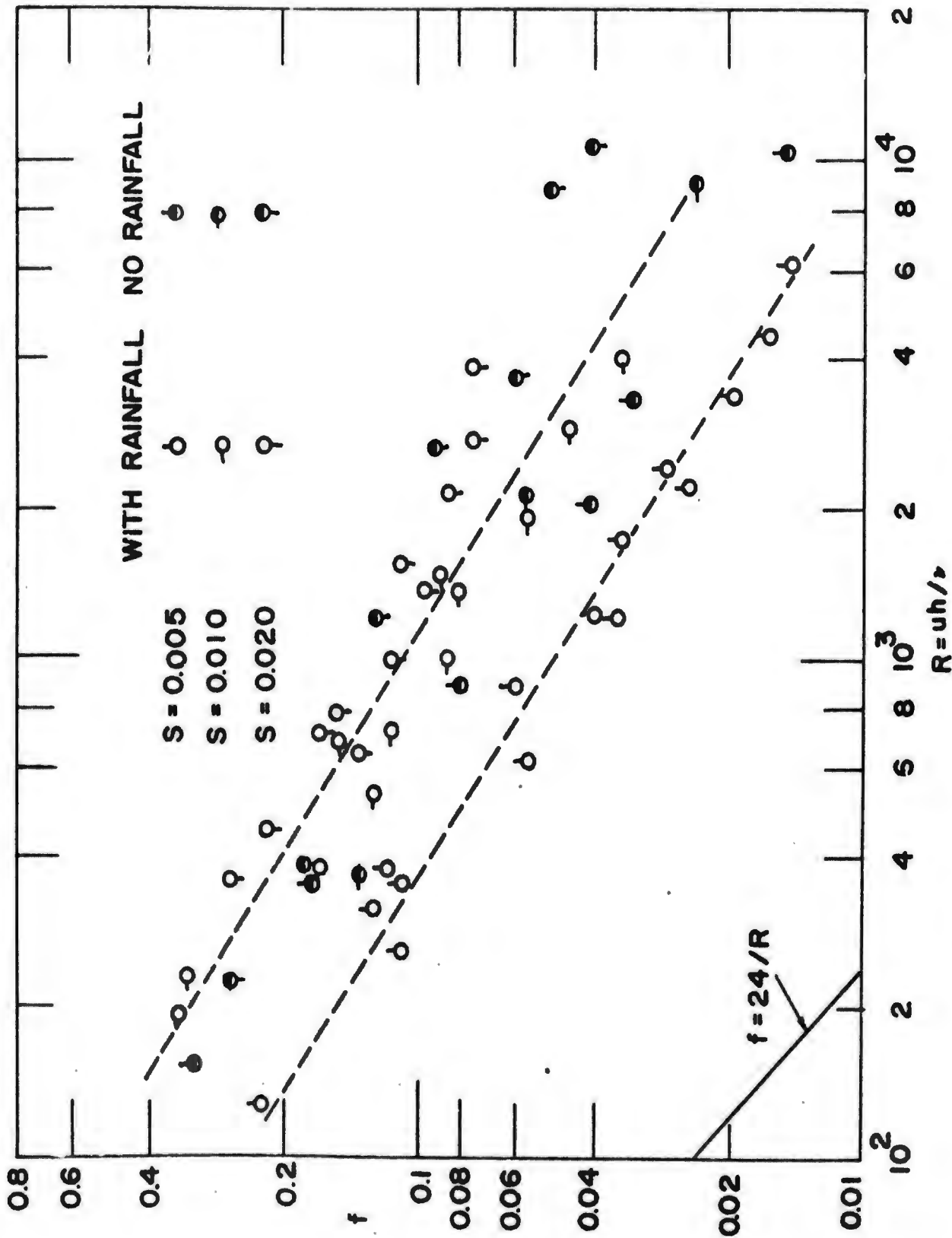


Fig. 3 Resistance to Sheet Flow on a Simulated Turf Surface.

RAINFALL INTENSITY  $\sigma$

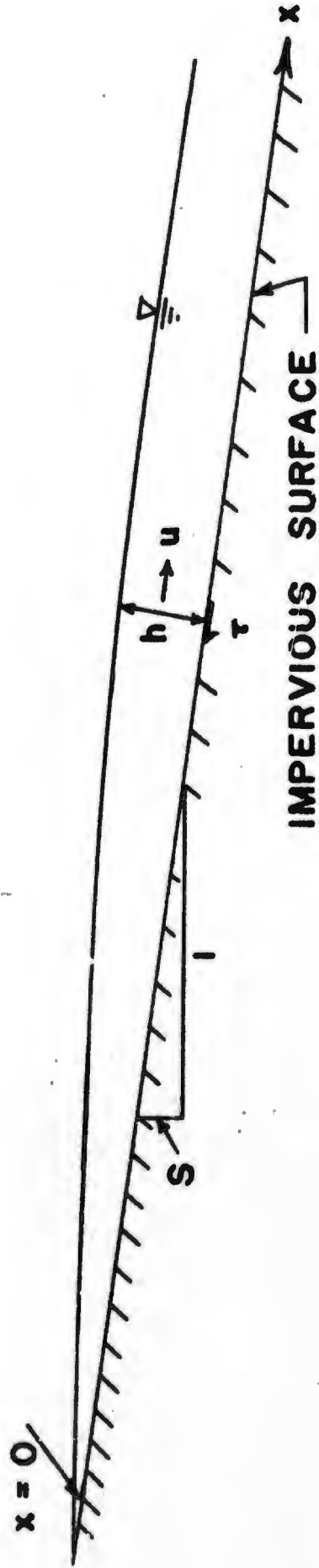


FIG. 4 DEFINITION SKETCH

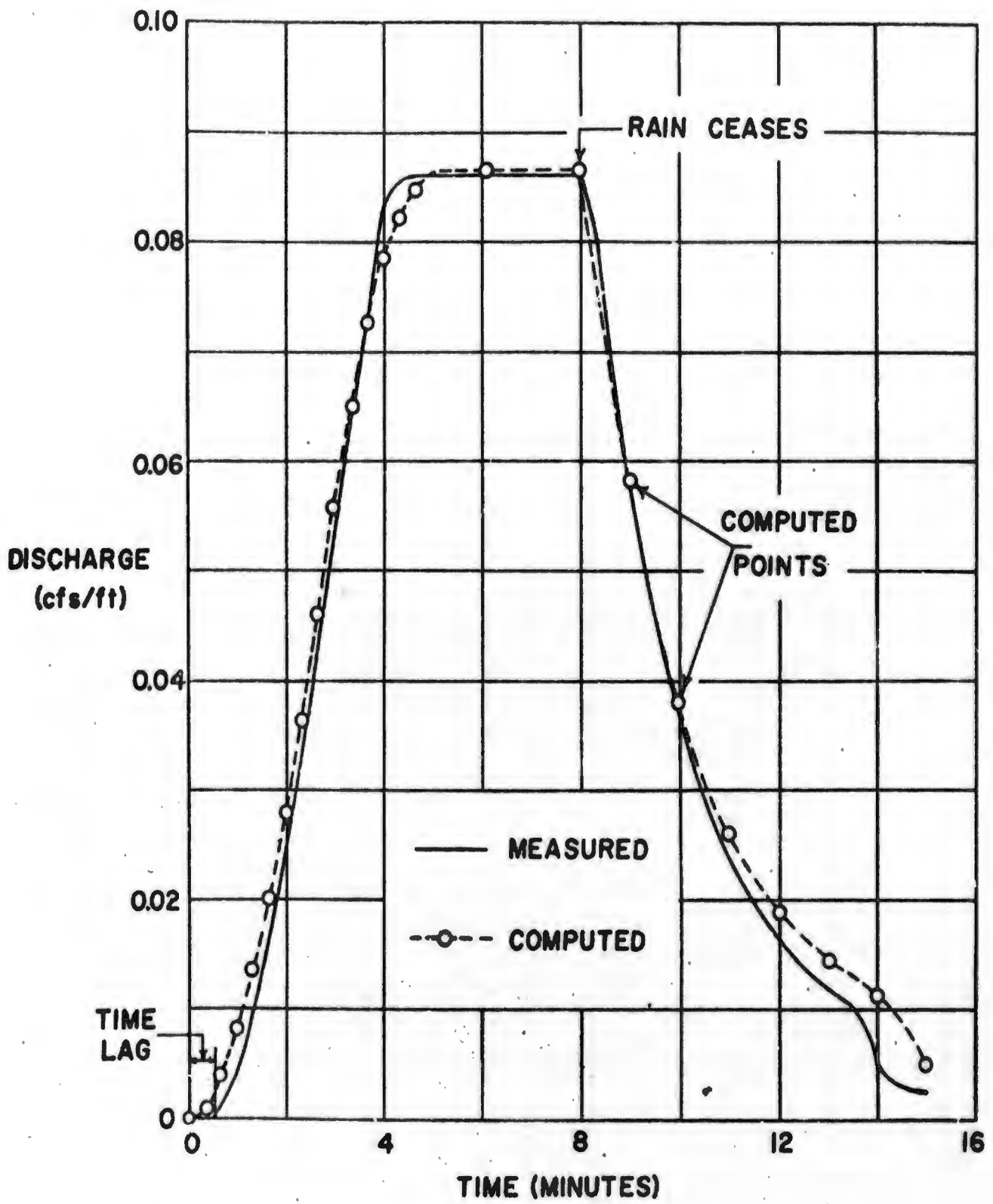


FIG. 5 RUNOFF HYDROGRAPHS, CASE 1,  $S = 2\%$ ,  $\sigma = 7.44$  in/hr.

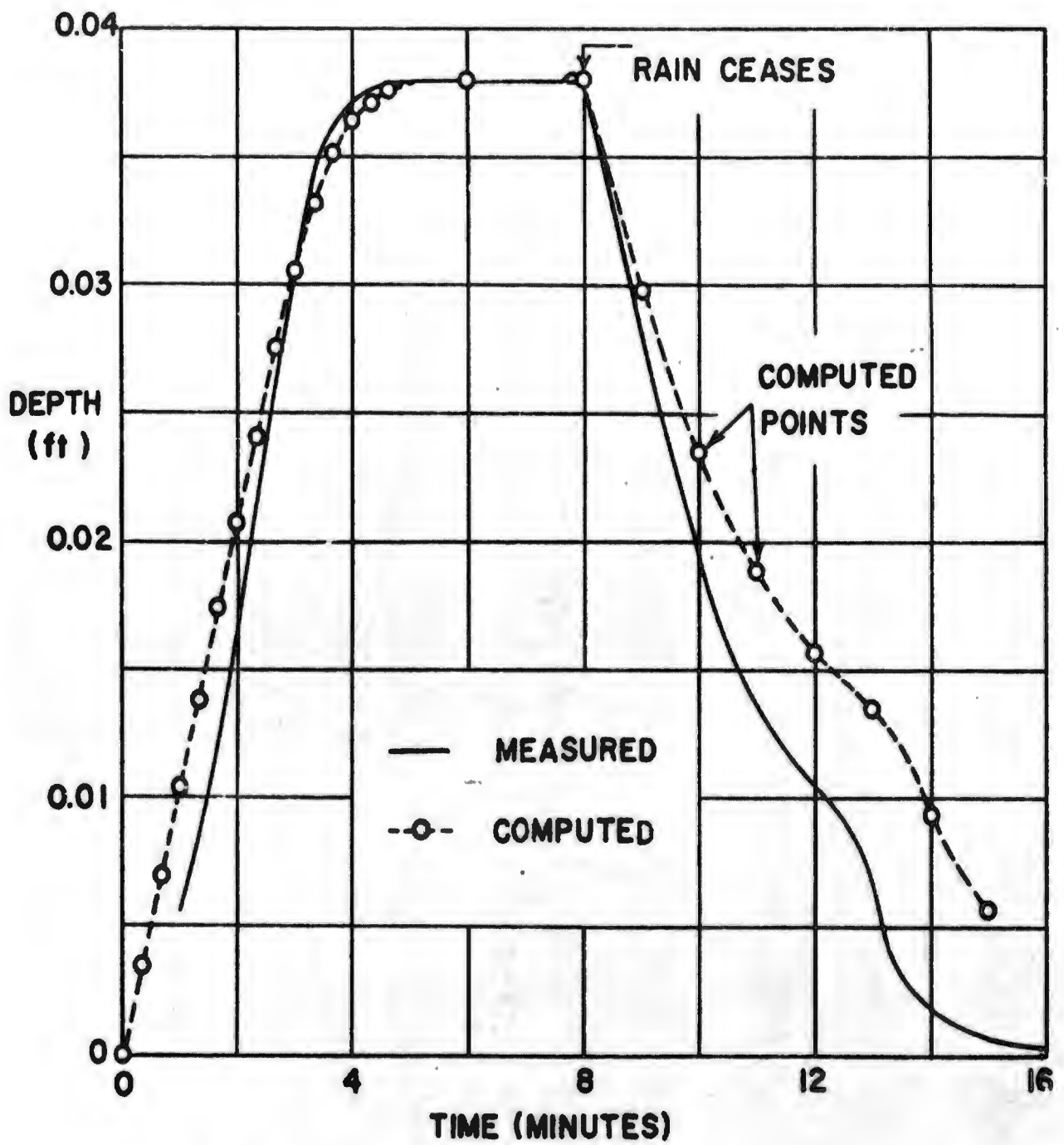


FIG. 6 DEPTH HYDROGRAPHS, CASE 1,  $S=2\%$ ,  $\sigma=7.44$  in/hr,  
 $x=467$  ft.

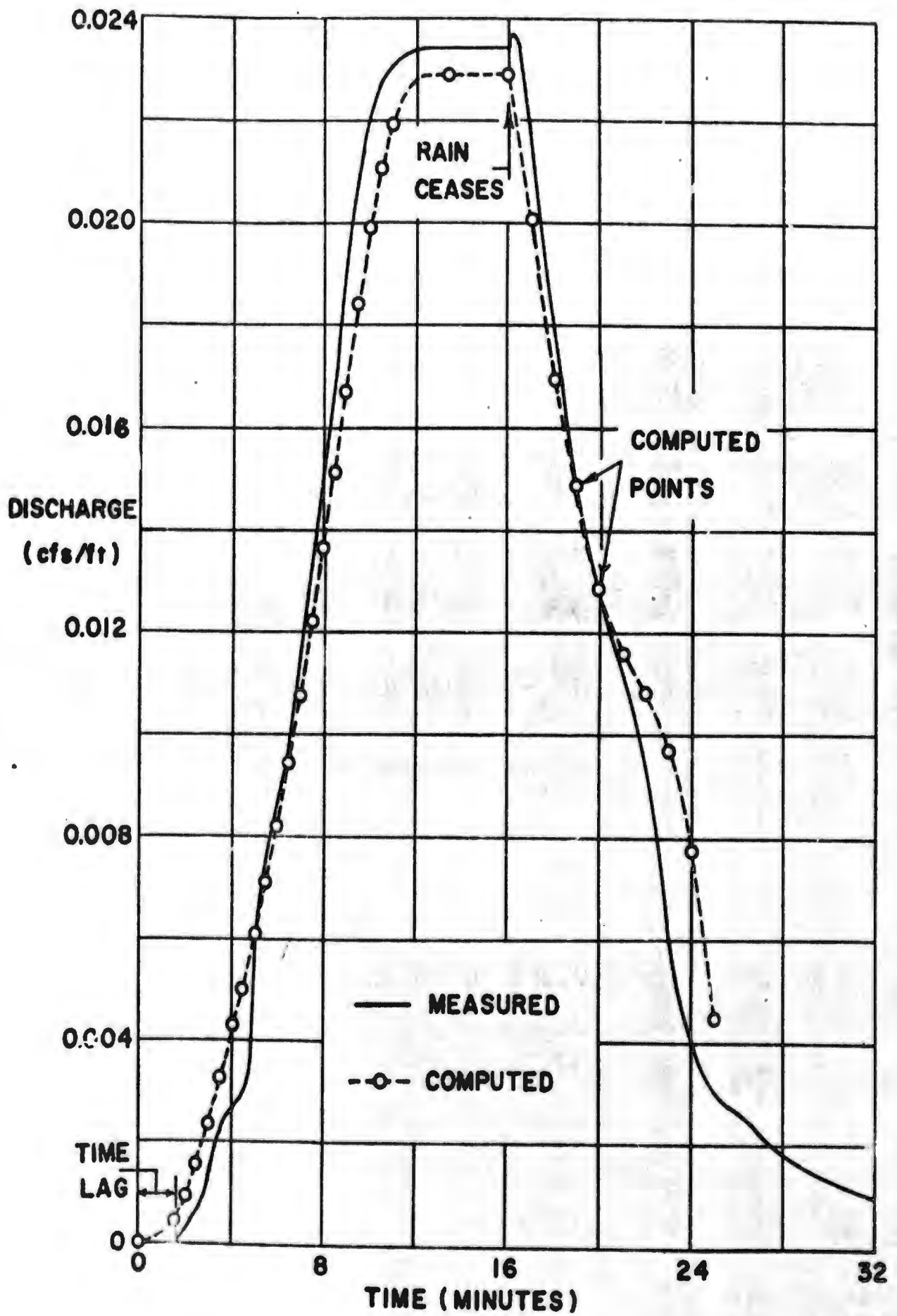


FIG. 7 RUNOFF HYDROGRAPHS, CASE II,  $S = 0.5\%$ ,  $\sigma = 1.98$  in/hr.

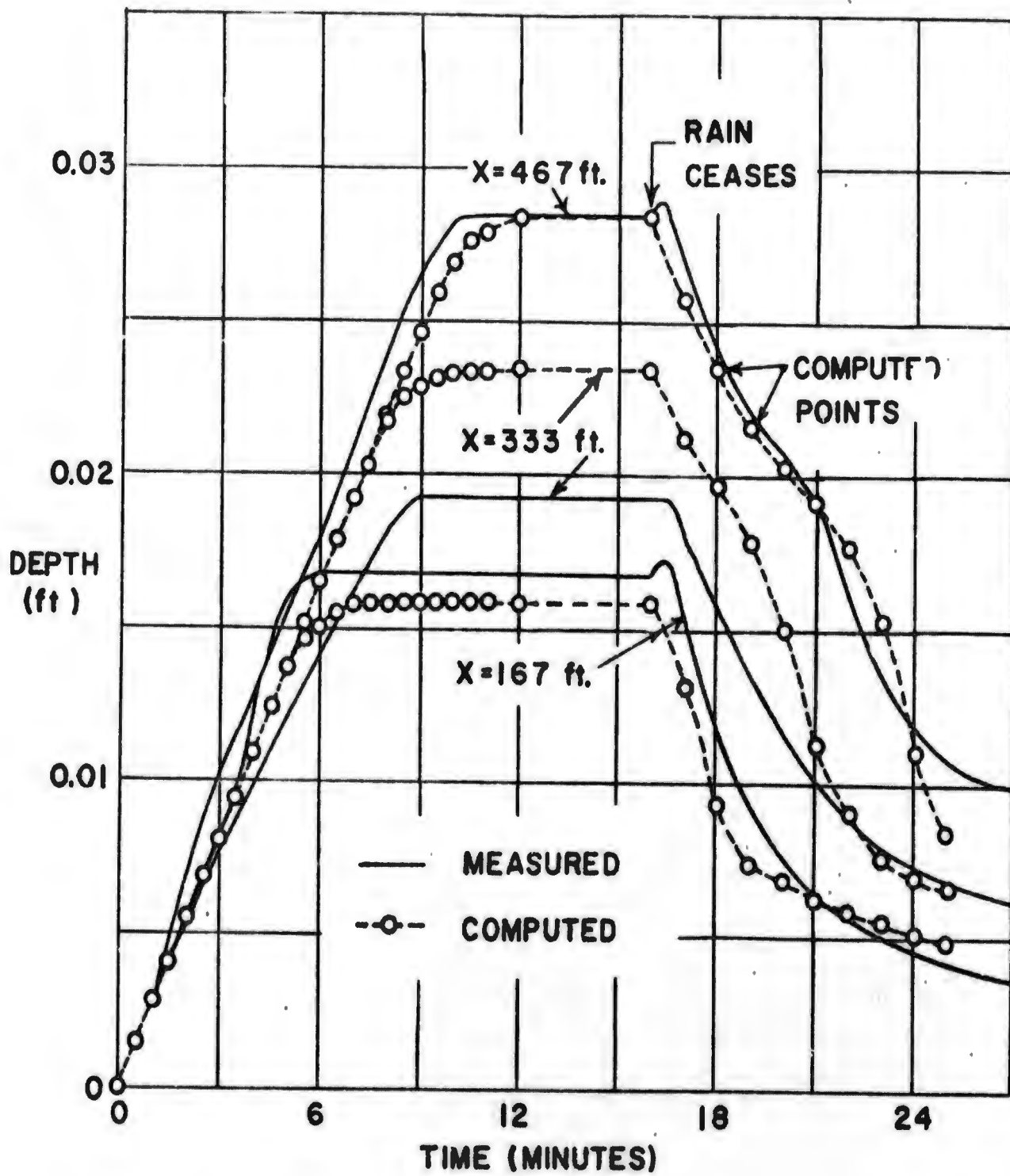


FIG. 8 DEPTH HYDROGRAPHS, CASE II,  $S = 0.5\%$ ,  $\sigma = 1.98$  in/hr.

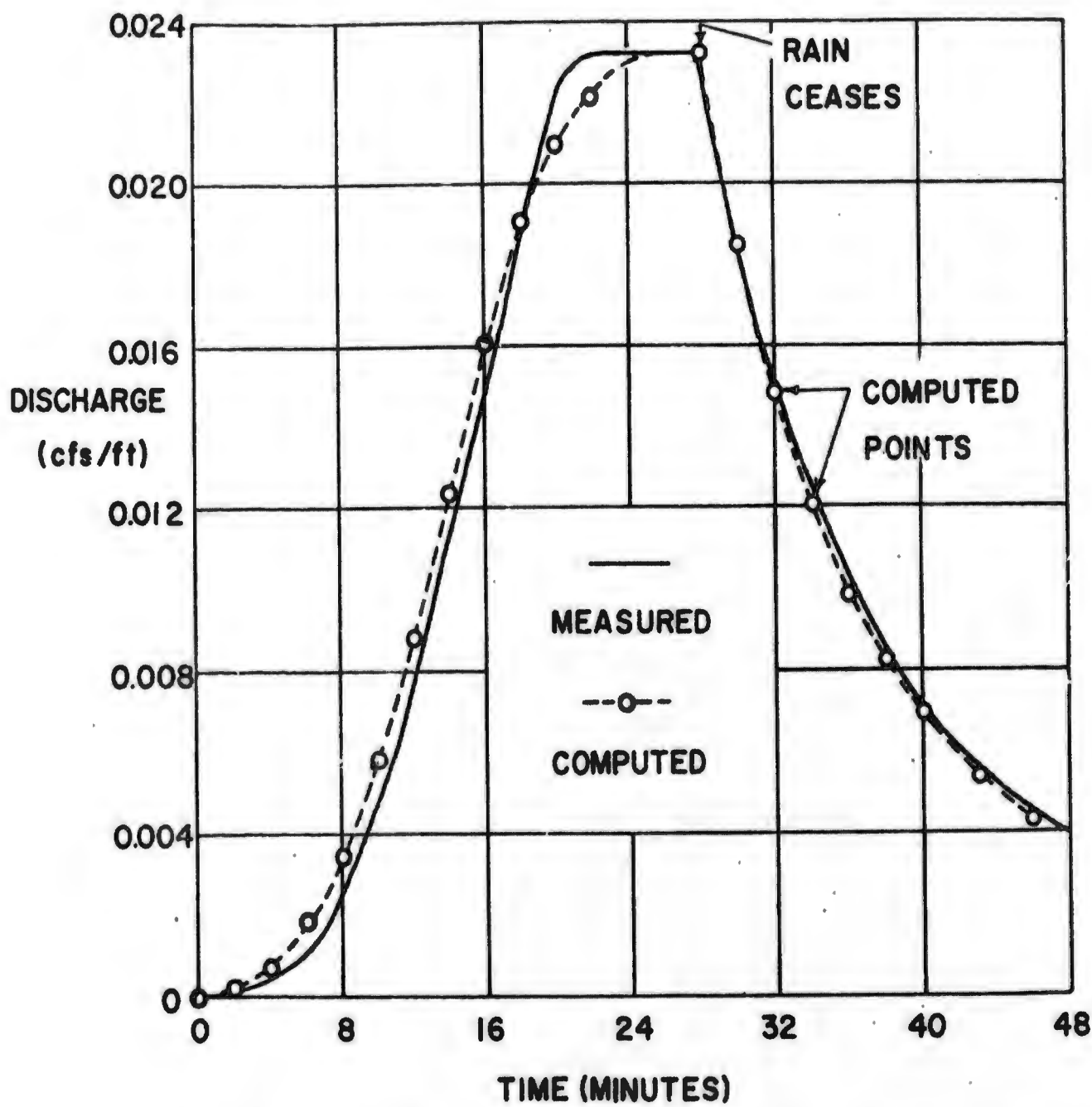


FIG. 9 RUNOFF HYDROGRAPHS, CASE III,  $S = 0.5\%$ ,  $\sigma = 2.00$  in/hr, SIMULATED TURF SURFACE.

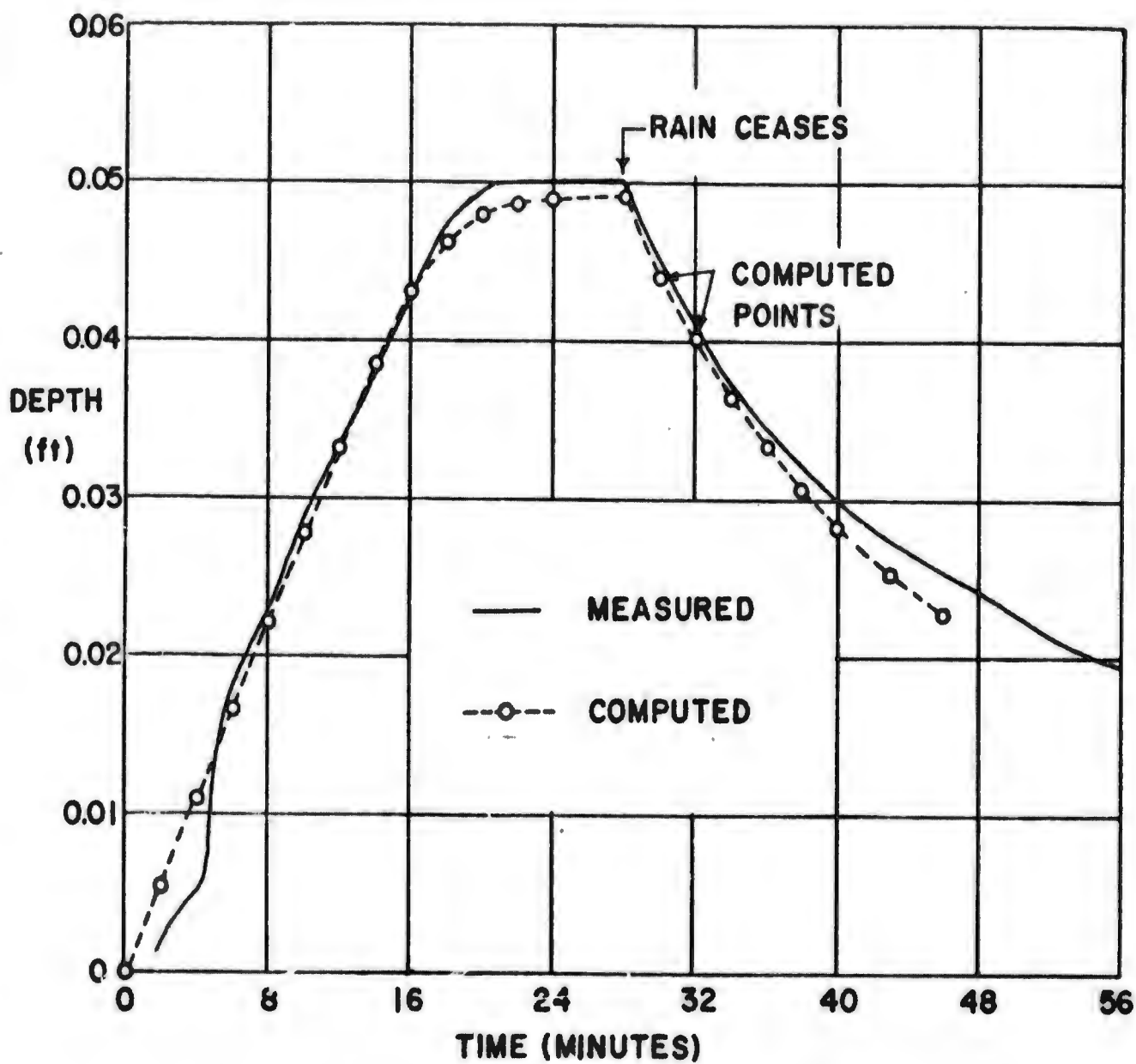


FIG. 10 DEPTH HYDROGRAPHS, CASE III,  $S = 0.5\%$ ,  $\sigma = 2.00$  in/hr,  $x = 467$  ft, SIMULATED TURF SURFACE.

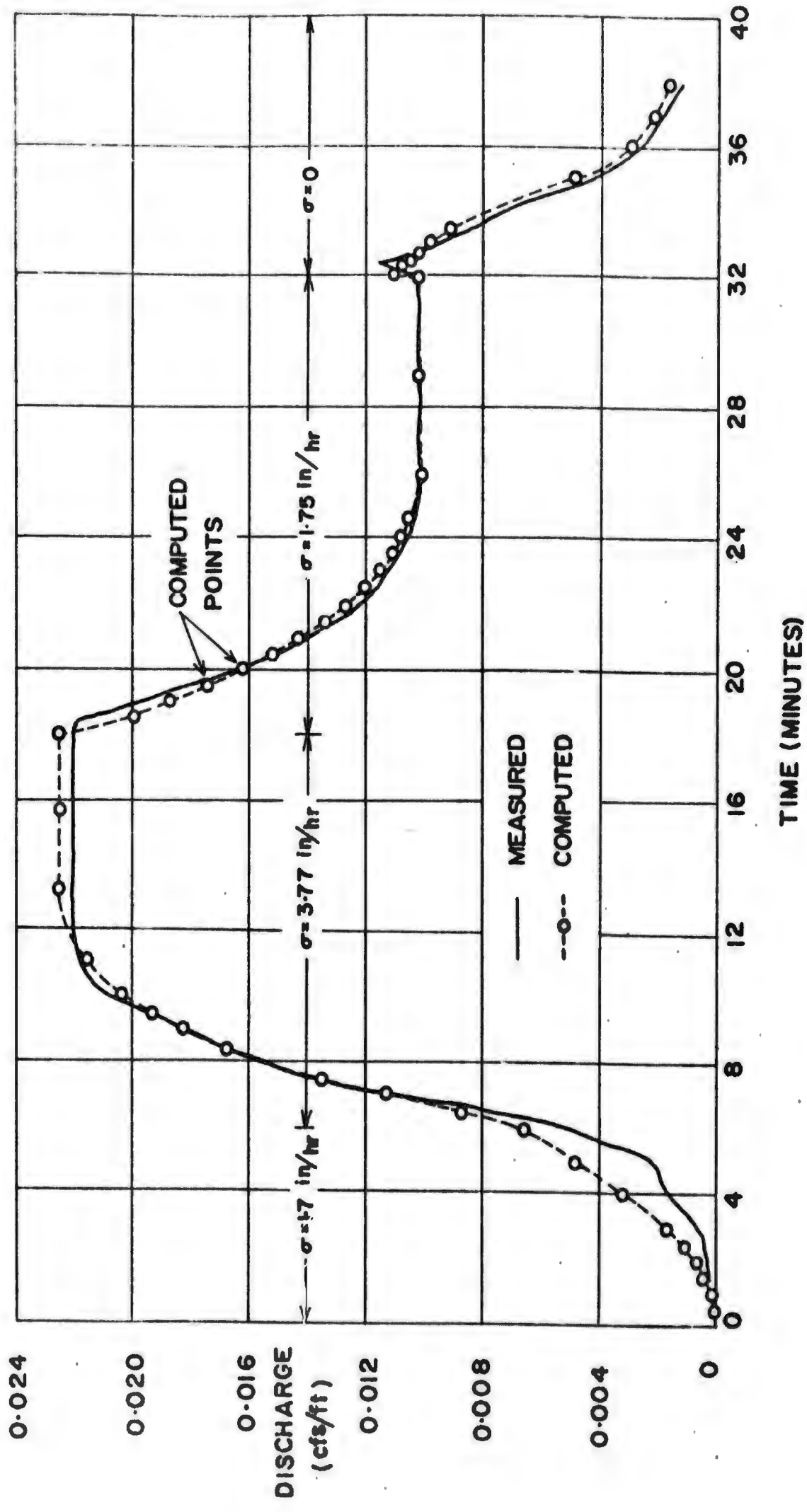


FIG. 11 RUNOFF HYDROGRAPHS, CASE IV, S = 0.5%, x = 252 ft.

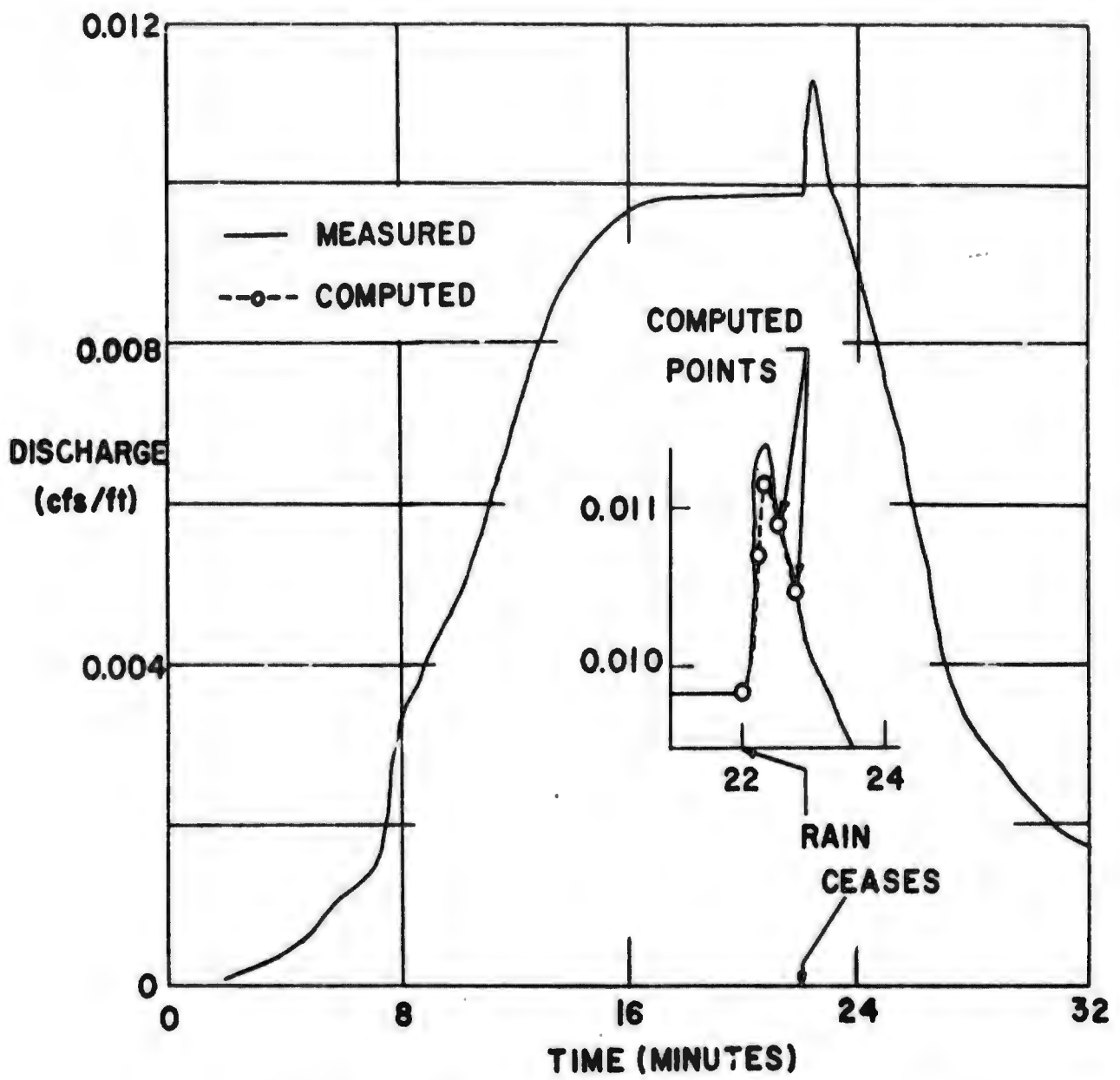


FIG. 12 AN EXAMPLE OF A PIP ON RUNOFF HYDROGRAPHS,  
 $S = 0.5\%$ ,  $\sigma = 0.851$  in/hr.

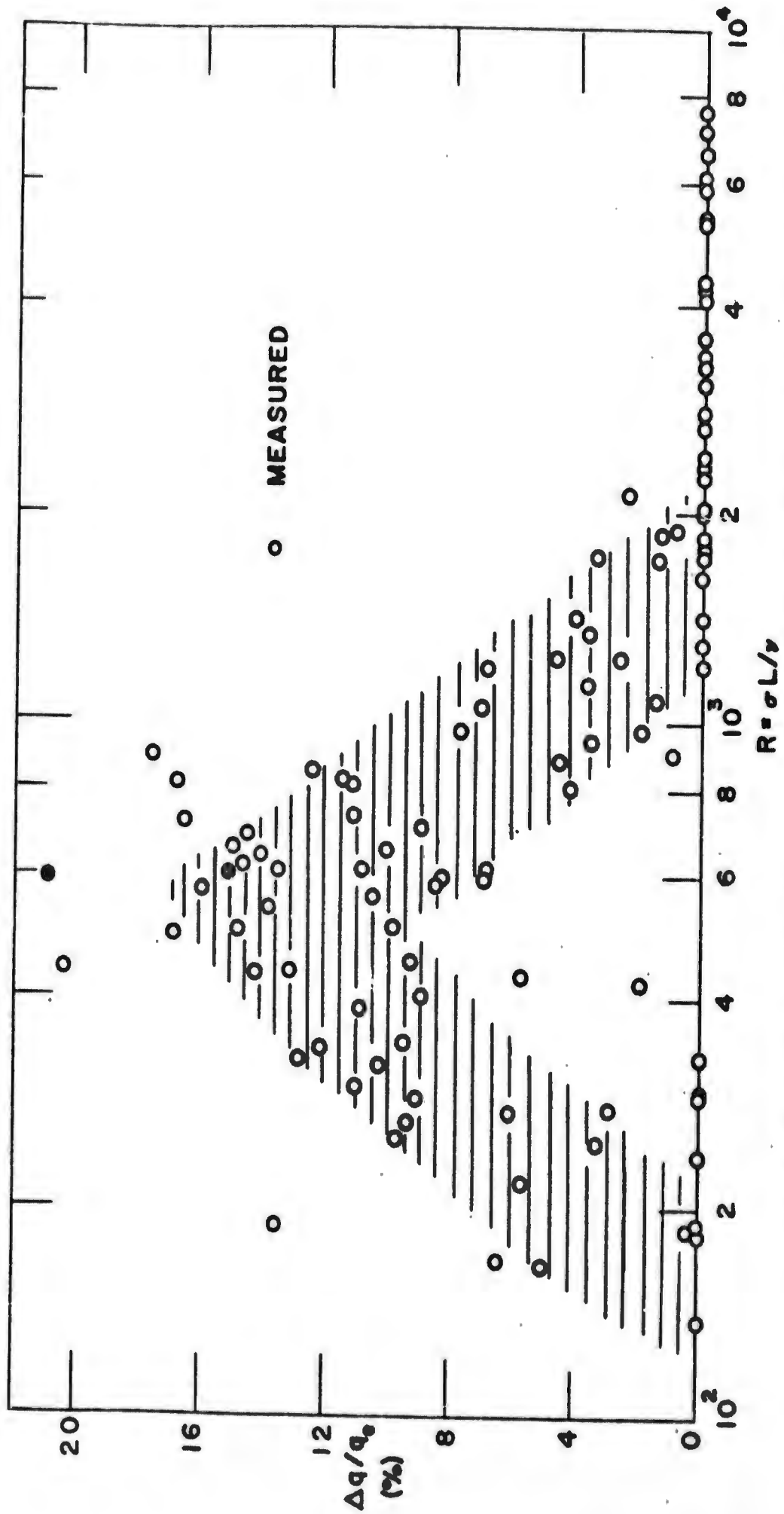


FIG.13 RELATIVE HEIGHT OF PIP AS A FUNCTION OF REYNOLDS NUMBER